THE JOURNAL OF PHYSICAL CHEMISTRY B

Article

pubs.acs.org/JPCB

Inhibitor-Induced Conformational Shifts and Ligand-Exchange Dynamics for HIV-1 Protease Measured by Pulsed EPR and NMR Spectroscopy

Xi Huang,[†] Ian Mitchelle S. de Vera,[†] Angelo M. Veloro,[†] Mandy E. Blackburn,[†,‡] Jamie L. Kear,[†,§] Jeffery D. Carter,[†] James R. Rocca,[∥] Carlos Simmerling,[⊥] Ben M. Dunn,[#] and Gail E. Fanucci*[,†]

[†]Department of Chemistry, University of Florida, P.O. Box 117200, Gainesville, Florida 32611, United States

[∥]Advanced Magnetic Resonance Imaging and Spectroscopy Facility, McKnight Brain Institute, and [#]Department of Biochemistry and Molecular Biology, University of Florida, Gainesville, Florida 32610, United States

[⊥]Department of Chemistry, Stony Brook University, Stony Brook, New York 11794, United States

Supporting Information

ABSTRACT: Double electron−electron resonance (DEER) spectroscopy was utilized to investigate shifts in conformational sampling induced by nine FDA-approved protease inhibitors (PIs) and a nonhydrolyzable substrate mimic for human immunodeficiency virus type 1 protease (HIV-1 PR) subtype B, subtype C, and CRF_01 A/E. The ligand-bound subtype C protease has broader DEER distance profiles, but trends for inhibitor-induced conformational shifts are comparable to those previously reported for subtype B. Ritonavir, one of the strong-binding inhibitors for subtypes B and C, induces less of the closed conformation in CRF_01 A/E. $^{1}H-^{15}N$ heteronuclear single-quantum coherence (HSQC) spectra were acquired for each protease construct titrated with the same set of inhibitors. NMR $^{1}H-^{15}N$ HSQC titration data show that inhibitor residence time in the protein binding pocket, inferred from resonance exchange broadening, shifting or splitting correlates with the degree of ligand-induced flap closure measured by DEER spectroscopy. These parallel results show that the ligand-induced conformational shifts resulting from protein−ligand interactions characterized by DEER spectroscopy of HIV-1 PR obtained at the cryogenic temperature are consistent with more physiological solution protein−ligand interactions observed by solution NMR spectroscopy.

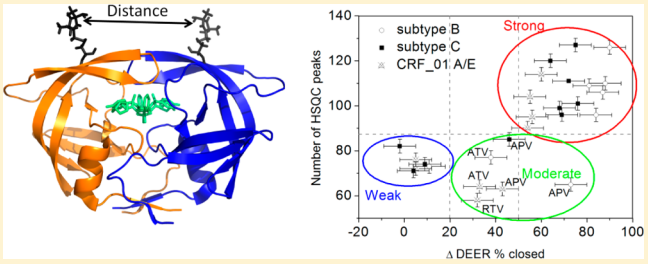

INTRODUCTION

Human immunodeficiency virus type 1 protease (HIV-1 PR), a homodimeric aspartic protease consisting of 99 amino acids in each subunit, is an essential enzyme necessary for the generation of mature, infectious virus particles. Since 1995, HIV-1 PR has served as a successful target in therapeutic regimens that employ protease inhibitors (PIs). However, the emergence of amino acid substitutions as naturally evolving polymorphisms and drug-selected mutations has reduced the effectiveness of several inhibitors, leading to failure of highly active antiretroviral therapy (HAART).[1−4]

HIV-1 is categorized into different groups, subtypes, and circulating recombinant forms (CRFs). The genomes of HIV-1 subtypes contain between 10% and 30% sequence variation, including variations in the protease gene.[2,5] Among the 34 million people infected worldwide, over 23 million live in Africa.[6] HIV-1 subtype C, the prevalent African variant, contains 30% genomic variation relative to subtype B,[7] which is the predominant variant in western Europe and North America. The prevalent subtype in south and southeast Asia, where 4 million people are living with HIV-1 infection, is CRF_01 A/E.[8,9] Given that current FDA-approved PIs are developed with subtype B as the therapeutic target, it is not surprising that naturally occurring polymorphisms in other subtypes lead to 2- to 7-fold lower inhibitor binding affinity.[10,11] Even though this decrease is modest and does not necessarily result in drug resistance, certain polymorphisms have been shown to amplify the drug-resistant effects of subsequent mutations.[10−12] Given that access to the active-site cavity is modulated by two β-hairpins, termed the flaps,[13] many mutations confer drug resistance by altering HIV-1 PR flap heterogeneity[14−16] and dynamics.[17,18] Thus, an understanding of how the polymorphisms alter protein structure, flexibility, and interaction with PIs could provide insights for the design of next-generation PIs to tailor-fit particular subtypes or circulating recombinant forms.

Site-directed spin labeling (SDSL) pulsed electron paramagnetic resonance (EPR) spectroscopy, specifically double electron−electron resonance (DEER) spectroscopy, is a spectroscopic method that has been used to monitor

Received: August 17, 2012
Revised: November 20, 2012
Published: November 20, 2012

   dx.doi.org/10.1021/jp308207h | J. Phys. Chem. B 2012, 116, 14235−14244

conformational ensemble sampling in apo and inhibitor-bound HIV-1 PR.[14,16,19−21] Because HIV-1 PR is a homodimer, substitution of lysine at position 55 with a cysteine, designated as K55C/K55C′, in the flap of each monomer, generates sites for attachments of nitroxide radical labels. The spin labels at these sites serve as a pair of reporters for DEER distance measurements (Figure 1). The magnitude of the magnetic

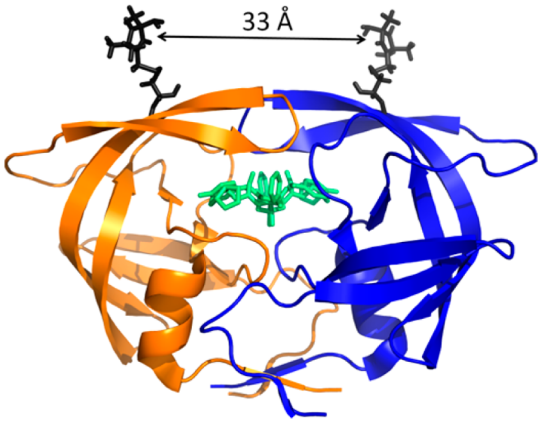

Figure 1. Ribbon diagram of CRF_01 A/E (PDB file 3LZS) protease in complex with Darunavir (colored in green). MTSL spin probes (K55R1) are incorporated in silico by MMM 2011.2 and rendered as gray sticks. The distance between spin labels is expected from modeling to be ∼33 Å. Each monomer of HIV-1 PR is rendered in a different color for clarity.

dipolar coupling of the two spins, which is inversely proportional to the cubic distance between the two spins,[22,23] is obtained from Tikhonov regularization (TKR) methods of the background-subtracted DEER echo curves and subsequently utilized to produce distance profiles.[22] By using site K55C/K55C′ labeled with methanethiosulfonate (MTSL) as a reporter of HIV-1 protease conformational ensembles, we have developed a model that decomposes the distance distribution profiles into nominally four protease conformations, namely curled/tucked, closed, semiopen, and wide-open conformations.[14,16] Our previous work has also shown that amino acid sequence variations among subtypes,[14] as well as drug-pressure-selected substitutions,[16] alter the conformational sampling ensemble. Moreover, the addition of inhibitors to subtype B and MDR769, a multidrug resistant sequence, was shown to induce shifts in the conformational ensemble to the closed conformation.[19,21]

Although SDSL-DEER spectroscopy provides direct information about distances that might not be readily attainable by other biophysical methods, the technique is often criticized for lack of physiologically relevant conditions. One of these is the requirement of cryogenic temperatures (20−80 K) to prolong the phase memory relaxation time (T_m). Another is the use of glassing agents for freezing, which can alter the thermodynamic properties of the system and inadvertently act as osmolytes.[24] A third is the effect of the freezing rate on the thermodynamic equilibrium of conformational sampling distributions.[25] Consequently, questions are often raised regarding whether and how an induced conformational shift in the presence of a ligand is altered by sample freezing and the presence of cosolutes, which are variations from physiological conditions.

With regard to HIV-1 PR, we have previously shown that various osmolytes do not alter the conformational sampling of apo HIV-1 PR.[26] In this work, to address the effects of temperature on relating the effects of protein−ligand binding on conformational shifts determined with DEER spectroscopy and solution binding equilibria, we utilized solution NMR spectroscopy to examine protein−ligand interactions in solution under more physiologically relevant conditions. To this end, uniformly ^{15}N-labeled HIV-1 PR was titrated with inhibitors, and the backbone chemical shift and peak intensity perturbations were monitored in the ^{1}H−^{15}N heteronuclear single-quantum coherence (HSQC) spectra. This method enables the approximation of inhibitor residence time and binding strength at room temperature, giving a relative estimate of the ligand-exchange dynamics, which we then show is related to the induced conformational shifts detected by DEER spectroscopy.

In both the NMR and EPR investigations, the total protein concentrations were similar (i.e., ∼50 μM dimer). The HSQC titration data support the results of SDSL-DEER measurements and suggest that pulsed EPR spectroscopy can be used to accurately characterize protein−inhibitor interactions in conformationally flexible enzyme systems such as HIV-1 PR. The results also indicate that the presence of the glycerol cosolute did not substantially perturb the trends in protein−ligand interactions. Additionally, in this study, parallel comparisons are made among subtype B, subtype C, CRF_01 A/E, and MDR769 flap distance profiles using SDSL-DEER spectroscopy and protease-inhibitor interaction dynamics using ^{1}H−^{15}N HSQC spectroscopy.

MATERIALS AND METHODS

Cloning and Site-Directed Mutagenesis. DNA samples that encode *E. coli* codon-optimized subtype B, subtype C, CRF_01 A/E, or MDR 769 HIV-1 PR were purchased from DNA 2.0 (Menlo Park, CA). Each construct was cloned into pET-23a vector (Novagen, Madison, WI) under the control of T7 promoter. Stabilized (Q7K, L33I, L63I) and inactive (D25N) constructs of subtype B (B_{si}), subtype C (C_{si}), CRF01_AE (AE_{si}), and inactive MDR 769 (MDR_i), with and without incorporated labeling sites (K55C) were made using the site-directed mutagenesis kit (Stratagene). Note that this procedure renders all mutations symmetrically applied to both subunits of the homodimer. Moreover, natural cysteine residues (C67A and C95A) in these constructs are mutated to alanine to ensure site-specific labeling and prevent nonspecific disulfide bond formation. The fidelity of the HIV-1 PR genes was confirmed by Sanger DNA sequencing (ICBR Genomics Facility, University of Florida). The complete amino acid sequences of the variants utilized in this study are given in the Supporting Information.

Protein Expression, Purification, and Spin Labeling for DEER Experiments. Protein expression, purification, and spin labeling were carried out as previously described[14,27] with the following modification: The pH of the inclusion bodies resuspension buffer used for anion exchange depends on the isoelectric point (pI) of a given construct. The buffer pH values for B_{si}, C_{si}, AE_{si}, and MDR_i 769 were adjusted to 9.30, 9.55, 9.20, and 8.80, respectively. MTSL was added in 3−4-fold molar excess to 8 μM HIV-1 PR homodimer in 10 mM Tris-HCl, pH 6.9, and the reaction was allowed to proceed in the dark for 12 h at 25 °C, 150 rpm. Excess free spin label was

dx.doi.org/10.1021/jp308207h | J. Phys. Chem. B 2012, 116, 14235−14244

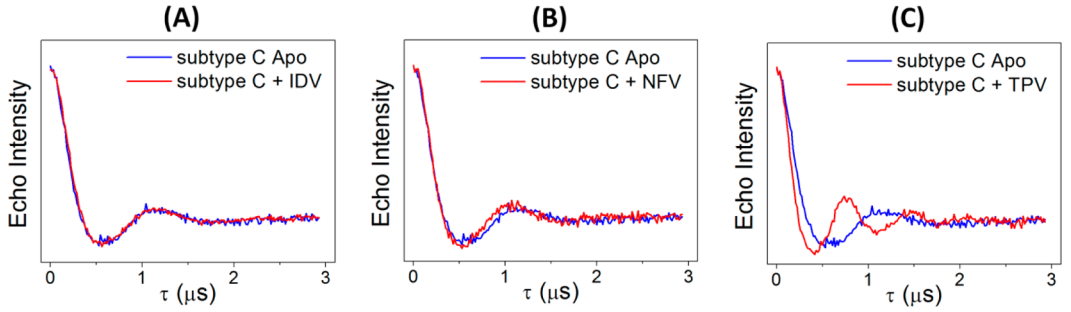

Figure 2. Comparison of background-subtracted time-domain dipolar modulation for subtype C apo (blue) and upon addition of inhibitors (red) (A) indinavir (IDV), (B) nelfinavir (NFV), and (C) tipranavir (TPV). The results are discussed within the text.

removed by buffer exchange into 2 mM NaOAc, pH 5.0, using a HiPrep 26/10 desalting column.

DEER Experiments and Sample Preparation. Protein samples consisted of 50 μM HIV-1 PR homodimer in 20 mM D_3-NaOAc/D_2O, pH 5.0, 30% D_8-glycerol. Inhibitor or substrate mimic was added at 3-fold excess to HIV-1 PR, and the solution was allowed to equilibrate at room temperature for 30−45 min. Samples were then transferred to a 4-mm quartz EPR tube and flash frozen in liquid nitrogen before the tube was inserted into the resonator. All pulsed EPR data were collected with a Bruker EleXsys E580 spectrometer equipped with the ER 4118X-MD-5 dielectric ring resonator at 65 K using a four-pulse DEER sequence,[28] as described in detail previously.[16] The DEER dipolar modulation curves were background-subtracted, high-pass-filtered, and converted to distance distribution profiles by Tikhonov regularization (TKR) using DeerAnalysis2008 (http://www.epr.ethz.ch/software/index).[29,30] The correct background subtraction level was determined using a self-consistent analysis procedure, where a series of Gaussian-shaped populations representing the nominal conformations of HIV-1 PR[14,19] with estimated relative percentages, full widths at half-maximum (fwhm), and most-probable distances were summed to reconstruct the distance profile using DeerSim. DeerSim is a Matlab-based program developed in our laboratory that is available upon request. Using this software, the dipolar evolution curve was regenerated from the summed Gaussian profile for comparison to the experimental background-subtracted data and TKR fit.[19] The optimal regularization parameter[31] was selected to guarantee conversion accuracy from the dipolar modulation curve to a TKR distance profile as previously described.[14,16,19] An example of full data analysis is provided in the Supporting Information.

Protein Expression and NMR Sample Preparation. DNA-encoding *E. coli* codon-optimized HIV-1 PR amino acid sequence B_{si}, C_{si}, AE_{si}, and MDR_i lacking the K55C substitution (i.e., K55) were cloned into pET-23a vector (Novagen, Madison, WI) under the control of T7 promoter. The vector was transformed in BL21*(DE3)pLysS *E. coli* cells (Invitrogen, Carlsbad, CA) and grown in modified minimal media with $^{15}NH_4Cl$ (Sigma-Aldrich, St. Louis, MO) as the sole nitrogen source. Overexpression of HIV-1 PR was induced when optical density of the culture was 0.8 (measured as absorbance at 600 nm), by adding isopropyl-β-D-thiogalactoside (IPTG) to a final concentration of 1 mM. Induction was allowed to proceed at 37 °C for 5−6 h. HIV-1 PR was purified from inclusion bodies as described previously.[14,19,26] [U−^{15}N] HIV-1 PR in the NMR sample was prepared at 40 μM homodimer in 2 mM D_3-NaOAc buffer at pH 5.0 with 10% D_2O and 0.1 mM DSS (4,4-dimethyl-4-silapentane-1-sulfonic acid) as an internal reference.

^{1}H−^{15}N HSQC Titration Experiments. Stepwise addition of inhibitors or substrate into 40−45 μM HIV-1 PR to a final concentration of 1:1.5 protease dimer-to-inhibitor ratio for subtype B, subtype C, and CRF_01 A/E was performed. This ratio was lowered to 1:1 for MDR 769. All ^{1}H−^{15}N HSQC spectra for [U−^{15}N] HIV-1 PR were acquired at 293 K using a Bruker Avance II spectrometer with a 5-mm TXI cryoprobe operating at 600 MHz (AMRIS Facility, University of Florida). Movements or disappearances of peaks were monitored by overlaying sequential ^{1}H−^{15}N HSCQ spectra. A protease dimer-to-inhibitor ratio of 1:1 was chosen for peak counting because significant amounts of free and bound protease are present under these conditions, thereby giving a more observable peak pattern change. NMRPipe[32] and Sparky (Goddard and Kneller, Sparky 3, University of California, San Francisco, CA) were used for processing and analysis of NMR data. Backbone chemical shift assignments were determined and reported in a previous publication.[33]

RESULTS AND DISCUSSION

DEER Data Analysis. The effects of inhibitors on the conformational sampling ensemble of subtype B, subtype C, and CRF_01 A/E were investigated by DEER spectroscopy. Distance distribution profiles for the K55R1/K55′R1 (Figure 1) pair located in the solvent-exposed flap sites were determined in the presence and absence of inhibitors. Figure 2 shows selected background-subtracted time-domain DEER modulation echo curves for subtype C, where the effects of inhibitor binding are readily apparent in the changes of the frequency of oscillations in the modulation curves. For example, addition of indinavir (IDV) causes almost no visual change in the DEER echo modulation curve when compared to that for the apo enzyme (Figure 2A). On the other hand, tipranavir (TPV) binding causes a strong change in the DEER signal compared to that for the apo state (Figure 2C). Specifically, TPV binding generates data with higher-frequency oscillations, indicative of a narrower distance profile. Additionally, for TPV, the first minimum in the DEER echo curve occurs sooner, indicative of a shorter most probable distance. These changes are consistent with a shift in the conformational sampling to the closed conformation.[19,34−36] In comparison, the data for nelfinavir (NFV) show a small but detectable change in the DEER signal (Figure 2B).

Deer echo curves were analyzed with the software package DeerAnalysis (http://www.epr.ethz.ch/software/index),[29,30] with TKR methods used to generate corresponding distance profiles. Figure 3 summarizes the resultant distance profiles

dx.doi.org/10.1021/jp308207h | J. Phys. Chem. B 2012, 116, 14235−14244

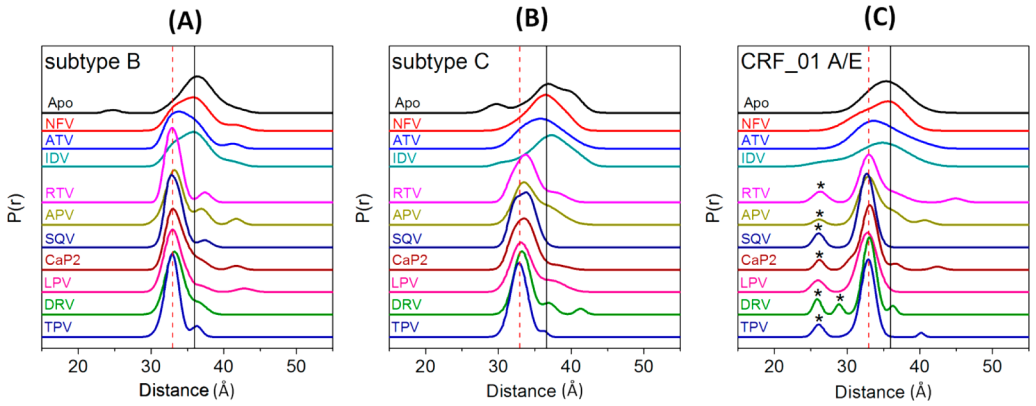

Figure 3. Distance distribution profiles for (A) subtype B, (B) subtype C, and (C) CRF_01 A/E in free (apo) and inhibitor-bound protease, where NFV = nelfinavir, ATV = atazanavir, IDV = indinavir, RTV = ritonavir, SQV = saquinavir, APV = amprenavir, CaP2 = substrate mimic, LPV = lopinavir, DRV = darunavir, TPV = tipranavir. Distances of 33 and 36 Å are indicated by the dashed red line and solid black line, and these distances are assigned to the closed and semiopen conformational ensembles, respectively.

obtained for subtype B,[19] subtype C, and CRF_01 A/E in the apo state and the presence of nine FDA inhibitors and the CAp2 nonhydrolyzable substrate mimic with sequence H-Arg-Val-Leu-r-Phe-Glu-Ala-Nle-NH2 (r = reduced). All background-subtracted time-domain modulation echo curves and complete data analyses can be found in the Supporting Information. The most probable distances for the apo constructs vary slightly. Distances of 36.2 ± 0.2, 36.9 ± 0.9, and 35.3 ± 0.2 Å were obtained for subtype B, subtype C, and CRF_01 A/E, respectively, providing an average most probable distance for the three constructs of 36.1 ± 0.8 Å (shown as solid vertical black lines in Figure 3 and summarized in Table 1). The DEER results show an average flap conformation in apo subtype C that is more "open" than that in subtype B, whereas for CRF_01 A/E, the flap conformation is more closed than that observed in subtype B. These trends are also seen in X-ray structures.[37,38] For subtype B, subtype C, and CRF_01 A/E, the presence of numerous inhibitors shifts the most probable distance to near 33 Å, with specific values ranging between 32.8 ± 0.2 and 33.8 ± 0.2 Å. For all three constructs with inhibitor IDV or NFV, the most probable distance decreases only slightly, if at all.

Table 1. Summary of Most Probable Distances (±0.2 Å) from DEER Distance Profiles of HIV-1PR Constructs

inhibitor	subtype B	subtype C	CRF_01 A/E
Apo	36.2	36.9	35.3
IDV	35.8	37.3	34.8
NFV	35.8	36.5	35.6
ATV	33.8	35.8	33.7
APV	33.2	33.5	32.9
LPV	33.0	33.1	32.8
DRV	33.2	33.3	33.0
RTV	32.9	33.7	33.0
TPV	32.9	32.8	32.9
SQV	32.8	33.8	32.7
CAp2	33.0	33.5	33.1

From modeling of X-ray structures and molecular dynamic simulations, a distance of 36 Å is assigned to the semiopen population, whereas a distance of 33 Å is consistent with the closed conformation.[14,34] In many cases, smaller peaks, located at 26−31 Å and 40−45 Å, are also seen in the DEER distance profiles in the apo state and in the presence of inhibitors. We assign these distances to the curled/tucked[39] and wide-open conformations,[40−42] respectively. Our assignments of these intraspin label distances of K55R1/K55′R1 to corresponding protein conformations is based on previous molecular dynamics simulation models and X-ray studies.[34,40,43,44] Interestingly, the presence of the curled/tucked state (marked by asterisks in Figure 3) is more pronounced in the DEER distance profiles for CRF_01A/E than for subtypes B and C. X-ray crystallography has shown that the salt bridge that forms between Glu35 and Arg57 in subtype B does not exist in CRF_01 A/E due to polymorphisms.[11,45] This altered salt bridge pattern might provide a structural underpinning for why an asymmetric open-like conformation is stabilized relative to the wide-open conformation in CRF_01 A/E.

During data analysis of DEER echo curves, it is important to carefully remove the effects that arise from intermolecular spin−spin interactions generating the background-subtracted echo curves as shown in Figure 2.[29] To achieve this goal, we used a self-consistent method of background subtraction in which we fit the TKR distance profiles from DeerAnalysis with a linear combination of Gaussian-shaped functions, which we then used to regenerate an echo curve.[19] The resultant curve was compared to our experimental data, and the process was repeated until a "match" was obtained. The significance of each population that comprises <20% of the total population was validated by suppressing that peak and comparing the theoretical curve to experimental data. By this means, we typically obtain certainty for distance peaks that comprise ≥5% of the total population when our signal-to-noise ratio is ≥25.[19] In general, up to four functions (i.e., populations) are necessary for adequate fitting of the TKR profile. These four populations we assign to the HIV-1 PR conformations mentioned above, namely, curled/tucked, closed, semiopen, and wide-open.[14,16]

The population analysis result for each construct is given in Figure 4, which shows the relative percentage, that is, the fractional occupancy, of each of these conformational states. These data show that, compared to subtype B, for the apo enzymes, subtype C contains a larger percentage of the wide-open state, whereas the conformational ensemble for CRF_01 A/E contains increased percentages of the closed and curled/tucked states with no wide-open conformation detectable within experimental error.[14] These differences in conformational ensemble fractional occupancy combine together in a

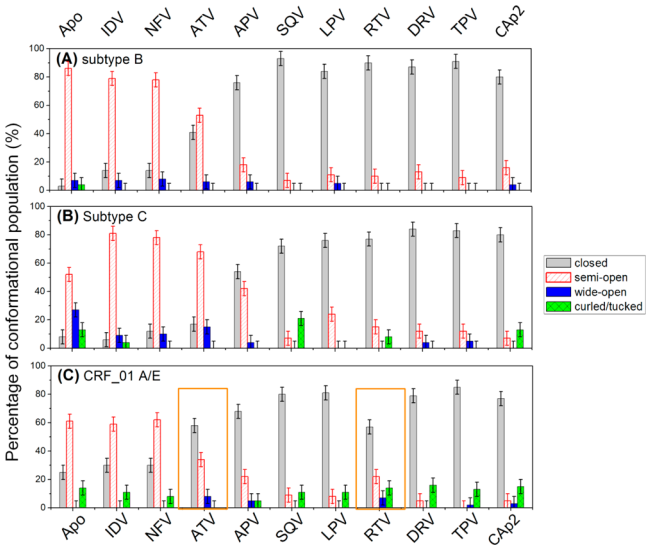

Figure 4. Relative percentage of each conformational population (i.e., fractional occupancy) for (A) subtype B, (B) subtype C, and (C) CRF_01 A/E in free (apo) and inhibitor-bound protease, with the following legend: closed (gray), semiopen (red striped), wide-open (blue), and curled/tucked (green hatched).

way that varies the most probable distances mentioned above, which again agrees with insights from X-ray structures of apo enzymes.[37,38,46]

Figure 4 also shows the relative populations of each variant in the presence of inihibitors. For all three variants, addition of inhibitors shifts the distance profiles in a manner such that the populations of the semiopen and wide-open states decrease with a concomitnant increase in the closed-state population. Interestingly, the curled/tucked population, the hypothesized asymmetric open-like state, remains unchanged within error throughout for all inhibitor binding in CRF_01 A/E. Furthermore, for CRF_01 A/E ATV, binding appears to induce more of a closed state than in subtype B or subtype C. On the other hand, RTV induces less of the closed conformation in CRF_01 A/E than in subtypes B and C. CAp2 is a nonhydrolysable substrate mimic inhibitor and is used as a positive control as it is expected to cause a shift to the closed state for each construct.

Based on the results of the DEER population analysis data, we defined the effects of inhibitors to induce flap closure in three categories, designated as weak, moderate, or strong, depending on the degree to which a ligand shifts the fractional occupancy to the closed state. To better quantify this variable, we define the parameter

$$\Delta c = \%c(\text{inhibitor}) - \%c(\text{apo}) \quad (1)$$

with $\%c$ designating the fractional occupancy of the closed state in the presence and absence of inhibitor. Weak inhibitors are categorized as those with $\Delta c < 20\%$, which also have a DEER distance profile with a most probable distance similar to that of the apo state (see Tables 1 and 2); indinavir (IDV) and nelfinavir (NFV) are considered weak for all three constructs. ATV is also considered weak for CRF_01 A/E. Inhibitors that have $\Delta c > 50\%$ are considered strong; saquinavir (SQV), lopinavir (LPV), darunavir (DRV), and tipranavir (TPV) are examples of inhibitors that are strong for all three constructs. For $20\% \leq \Delta c \leq 50\%$, inhibitors are classified as moderate. Figure 5 shows plots of Δc values for each construct; the dashed and dotted lines in the plots show the cutoff values for the classifications of weak, moderate, and strong. Table 2 summarizes the classification of inhibitors for each construct studied here and for MDR769, a multidrug-resistant construct that we recently investigated by DEER spectroscopy.[21] Figure 5D shows that, in general, the inhibitors induce similar or slightly smaller shifts to the closed state for subtype C and CRF_01 A/E than for subtype B.

Table 2. Summary of Induce-Flap-Closure Ability for Inhibitors on Different HIV-1 PR Constructs Based on the DEER Percentage Change in Flap Closed Conformation

	inhibitor category from DEER data		
HIV-1 PR construct	weak	moderate	strong
subtype B	IDV, NFV	ATV	APV, RTV, SQV, TPV, LPV, DRV
subtype C	IDV, NFV, ATV	APV	RTV, SQV, TPV, LPV, DRV
CRF_01 A/E	IDV, NFV	ATV, APV, RTV	SQV, TPV, LPV, DRV
MDR 769	IDV, NFV, ATV, APV, RTV, SQV,		TPV, LPV, DRV

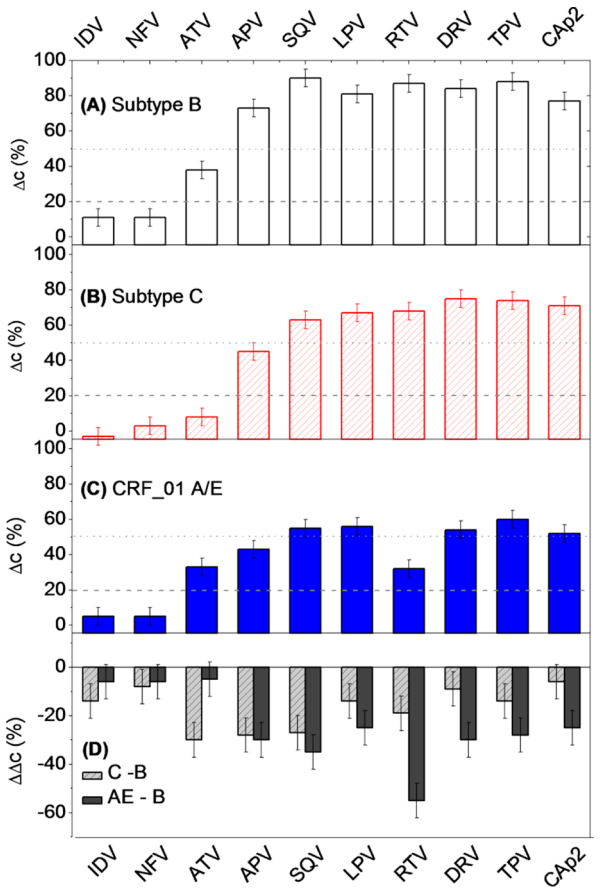

Figure 5. Change in the fractional occupancy of the closed state, Δc, for inhibitor-bound proteases (A) subtype B, (B) subtype C, and (C) CRF_01 A/E, where Δc = percentage closed (inhibitor) − percentage closed (apo). (D) Plot of the change in fractional occupancy of the closed state, $\Delta\Delta c$, between variants and subtype B, where $\Delta\Delta c = \Delta c(\text{variants}) - \Delta c(\text{subtype B})$. The dotted and dashed lines mark the boundaries for the classification of weak, moderate, and strong interactions taken as 20% and 50%, respectively.

dx.doi.org/10.1021/jp308207h | J. Phys. Chem. B 2012, 116, 14235−14244

^{1}H−^{15}N HSQC Titration Experiments. The exchange dynamics of inhibitor−protein interactions were interrogated by ^{1}H−^{15}N HSQC NMR experiments, where increasing concentrations of each PI were titrated into each HIV-1 PR variants. Because amide backbone chemical shifts are sensitive to changes in the local environment, such as inhibitor binding to a protein, the exchange dynamics of the inhibitors with protease can be assessed by monitoring shifts and broadening of the HSQC resonances. The type of change in the HSQC resonances (i.e., shift or broadening) is dictated by the exchange rate between unbound and bound species relative to differences in the chemical shifts of the bound and unbound state.[47] As illustrated in Figure 6, residues under slow exchange

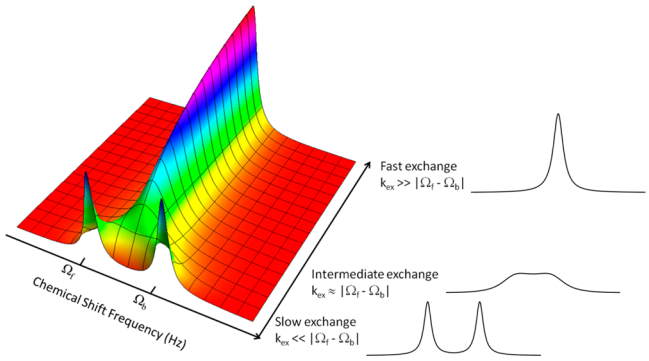

Figure 6. Simulated 1D NMR spectra of a two-site chemical exchange process. Ω_f and Ω_b are the chemical shifts at a ligand-free and ligand-bound protein site, respectively. k_{ex} is the exchange rate between the free and bound protein. To simplify, relaxation constants were set as $R_{2f} = R_{2b} = 10\ s^{-1}$, and the populations of free and bound protein were assumed to be equal ($p_f = p_b = 0.5$), with parameters $\Delta\omega = |\Omega_f - \Omega_b| = 120$ Hz and $k_{ex} = 0.1-1000\ s^{-1}$. Calculations were performed and graphics were prepared using Mathematica (Wolfram Research).

appear as two distinct resonances that represent the free and inhibitor bound states. Meanwhile, intermediate exchange with a ligand results in cross-peak broadening and possible disappearance. Finally, residues under fast exchange have a resultant resonance that appears at a weighted-average chemical shift, merging the free and bound states into a single HSQC cross-peak. One unique attribute of homodimeric proteins, such as HIV-1 PR, is the chemical shift degeneracy of residues for each monomer due to the C_2 symmetry in the apo enzyme. However, upon binding with an asymmetric ligand (all of the inhibitors utilized here are asymmetric), the residues for each monomer will sense disparate environments, leading to the observance of peak splitting for bound species in the HSQC spectra. In the situation of slow exchange coupled to lost degeneracy for the bound protease, the HSQC cross-peak for the affected residue can be split into as many as three separate resonances (two for each bound monomer and a degeneracy signal for the free protease).

To assess the effects of ligand binding to subtype B, subtype C, CRF_01 A/E, and MDR769, ^{1}H−^{15}N HSQC titration experiments were performed using nine FDA-approved inhibitors. Recently, we reported the backbone NMR chemical shift assignments for subtype C, CRF_01 A/E, and MDR 769.[33] The backbone assignments for subtype B were reported earlier by others.[48] Figure 7 shows representative ^{1}H−^{15}N HSQC spectra for free and selected inhibitor-bound subtype C protease samples. Throughout the course of titrations, chemical shift perturbations and signal intensities were measured for the resonances. As with the DEER experiments, we found the results from the NMR experiments to be grouped into categories; however, here, we only distinguish two, namely, fast/intermediate exchange and slow exchange. The PIs in the former category are characterized as those inhibitors that result in resonance disappearances or limited changes in the HSQC spectra as inhibitor is titrated to a 1:1 protease dimer/inhibitor ratio. Meanwhile, ligands in the slow category are designated by inducing resonance shifts or splittings in the HSQC spectra. A gradual decrease in the signal intensity or complete disappearance of the resonance signal suggests that the ligand-binding exchange rate in the protease−ligand (i.e., PL) equilibrium (eq 2) is in the intermediate exchange regime of NMR time scale or when $k_{ex} \approx |\Omega_f - \Omega_b|$, where Ω_b is the frequency of a resonance in the presence of a ligand and Ω_f is the frequency in the free protein. On the other hand, resonance shifting and splitting corresponds to slow exchange ($k_{ex} \ll |\Omega_f - \Omega_b|$). The opposite case is described as fast exchange ($k_{ex} \gg |\Omega_f - \Omega_b|$), where the resonances shift and coalesce into a single signal.

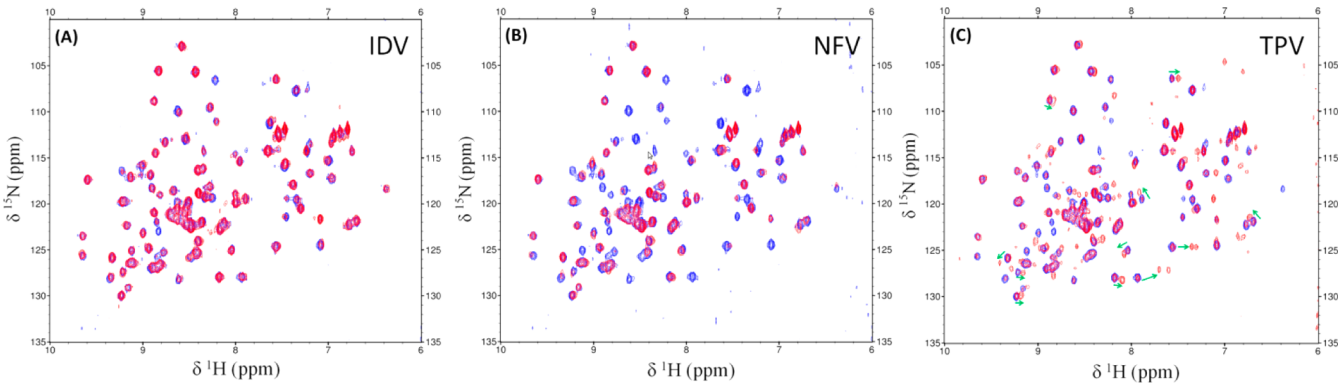

Figure 7. Selected ^{1}H−^{15}N HSQC spectra of HIV-1 PR subtype C in the apo (red) state and bound to 1:1 inhibitor/protein dimer (blue). Spectra were collected in 2 mM D_3-NaOAc buffer acquired at pH 5 and 20 °C. (A) Limited change was observed with addition of 1-fold IDV because of low binding affinity or fast exchange. (B) Titration of 1-fold Nelfinavir (NFV) causes at least 16 peaks to disappear as a result of fast/intermediate exchange. (C) Addition of 1-fold TPV causes several peaks to move and/or split as a result of slow exchange. Total peak number is seen to increase. The direction of peak movement is shown by the green arrows. Similar ^{1}H−^{15}N HSQC spectra were collected for subtype C, subtype B, CRF_01A/E, and MDR769 with inhibitors; data are given in the Supporting Information.

dx.doi.org/10.1021/jp308207h | J. Phys. Chem. B 2012, 116, 14235−14244

$$P + L \underset{k_{off}}{\overset{k_{on}}{\rightleftharpoons}} PL \qquad \text{where} \quad k_{ex} = k_{on}[L] + k_{off} \tag{2}$$

Figure 7 shows selected $^{1}H-^{15}N$ HSQC spectra overlain for unbound subtype C HIV-1 PR (blue) and inhibitor-bound protease for each category described above, namely, with IDV, NFV, and TPV (red). Subtype C bound to IDV shows minimal chemical shift perturbation compared to unbound protease, with only five resonance disappearances. These results suggest low binding affinity, which is consistent with fast exchange for most residues and translates to minimal perturbation of the HSQC resonances of the free protease. The lack of perturbations in the HSQC spectrum with IDV can also be understood by considering that, when the binding affinity is low, there are simply fewer protein molecules in the bound state that contribute to the total spectrum. When binding NFV with a 1:1 protease dimer/inhibitor ratio, ~16 cross-peaks disappear, indicating intermediate exchange. Intermediate exchange was also observed for ATV and APV. The HSQC splitting pattern in Figure 7C shows that, when subtype C is bound to TPV, cross-peaks shift and split, indicating slow exchange for this inhibitor. Peak splitting and shifting were also observed for inhibitors LPV, RTV, SQV, and DRV. Analogous HSQC spectra were acquired and analyzed for subtype B, CRF_01 A/E, and MDR769 with and without inhibitors. Representative HSQC spectra are provided in the Supporting Information. The results for categorizing inhibitors into a fast/intermediate or slow exchange regime with each construct are summarized in Table 3.

Table 3. Summary of Exchange Dynamics Assignments for Different HIV-1 PR Constructs in the Presence of Inhibitors Based on Their Impact on the HSQC Resonance Pattern

	inhibitor category based on HSQC data	
HIV-1 PR construct	fast/intermediate exchange	slow exchange
subtype B	IDV, NFV, ATV, APV	RTV, SQV, TPV, LPV, DRV
subtype C	IDV, NFV, ATV, APV	RTV, SQV, TPV, LPV, DRV
CRF_01 A/E	IDV, NFV, ATV, APV, RTV	SQV, TPV, LPV, DRV
MDR 769	IDV, NFV, ATV, APV, RTV, SQV	TPV, LPV, DRV

Comparison of Pulsed EPR and NMR Results. The effects of inhibitors on flap closure and exchange dynamics for various HIV-1PR constructs are summarized in Tables 2 and 3, respectively. As can readily be seen, the effects of inhibitors such as IDV, NFV, TPV, LPV, and DRV are unchanged in the two types of interactions. However, changes in inhibitor–protein interactions can be observed for inhibitors such as ATV, APV, RTV, and SQV. Specifically, RTV changes from slow exchange in subtypes B and C to fast/intermediate exchange with CRF_01 A/E and MDR769. The HSQC spectra for RTV-bound HIV-1 PR constructs can be found in the Supporting Information. SQV also changes from slow exchange to fast/intermediate exchange with MDR769. From the NMR perspective, these changes indicate weaker inhibitor interactions with the protein. This same "switch" can be seen among the DEER categories for inhibitor ability to induce flap closure. RTV and SQV are in the strong category for subtypes B and C. RTV moves to the moderate category for CRF_01 A/E, whereas both RTV and SQV move to the weak category for MDR769. The finding that RTV and SQV have weaker interactions with MDR769 is not surprising given that this drug resistance construct exhibits higher levels of resistance to most FDA-approved PIs, with the exception of DRV, TPV, and LPV.[49,50]

To correlate the relationship between flap closure and ligand dynamics, we plotted the number of HSQC cross-peaks against the fractional occupancy of the closed conformation from DEER analysis (Δc) for the various HIV-1 PR constructs (Figure 8). The grouping in the data shows the relationship between the ability of the inhibitors to induce the closed conformation and the ligand–protein exchange rate. In general, for the HIV-1 PR constructs investigated here, inhibitors that are classified as weak or moderate according to DEER distance profiles consistently give HSQC spectra that contain little to no change or resonance disappearance, that is, they exhibit fast/intermediate exchange. The addition of the DEER-induced conformational shift characterization of weak, moderate, and strong allows for a second dimension in the separation of protein–inhibitor interactions that are not discriminated within the NMR experiments. On the other hand, inhibitors described as strong for inducing a predominantly closed population cause shifts or splitting in the HSQC resonances. This suggests that weak or moderate inhibitors, which render the protease flap conformation to be predominantly semiopen, have shorter residence time (i.e., fast/intermediate exchange) in the active-site pocket or occupy the pocket with increased dynamic mobility but do not escape.[51,52] Meanwhile, strong inhibitors, which promote flap closure, correspond to PIs that have less dynamics in the binding cleft (i.e., slow exchange). The only exception to these trends appears to be APV with both subtype B and MDR769, where DEER results characterize the degree of flap closure as strong but NMR experiments indicate that the inhibitor is experiencing intermediate/fast exchange. This discrepancy might originate from the smaller size of APV, or the solutes might alter the interactions of this inhibitor.

Nevertheless, the relationship observed between induced conformational shifts observed with DEER spectroscopy and the ligand-exchange dynamics inferred from solution NMR spectroscopy indicate that the presence of glycerol and the freezing of samples required for DEER spectroscopy do not artificially perturb protein–ligand interactions in HIV-1 PR. Additionally, the findings indicate that DEER spectroscopy is a suitable means for interrogating protein–ligand interactions, capable of producing results similar to those obtained from standard NMR methods. Although both NMR and DEER spectroscopies are suitable for the small water-soluble HIV-1 PR, DEER spectroscopy can be utilized on protein systems and macromolecular complexes that are too large or too heterogeneous for solution NMR investigations. In this way, the studies on HIV-1 PR presented here also represent a simple model system for investigating the limitations and capabilities of DEER spectroscopy.

Biological Significance: Relating Δc to K_i Values. Given that all of our DEER data and the NMR data were collected on protease samples rendered inactive by the D25N mutation, we wanted to assess the relationship of these results to the inhibition constants determined with active HIV-1 PR enzymes. Because HIV-1 PR is a protease that will undergo autoproteolysis,[46] which can complicate data acquisition and interpretation in both EPR and NMR applications,[48] we chose the inactive enzyme for our spectroscopic studies due to enhanced protein stability. Although the catalytic aspartic acid

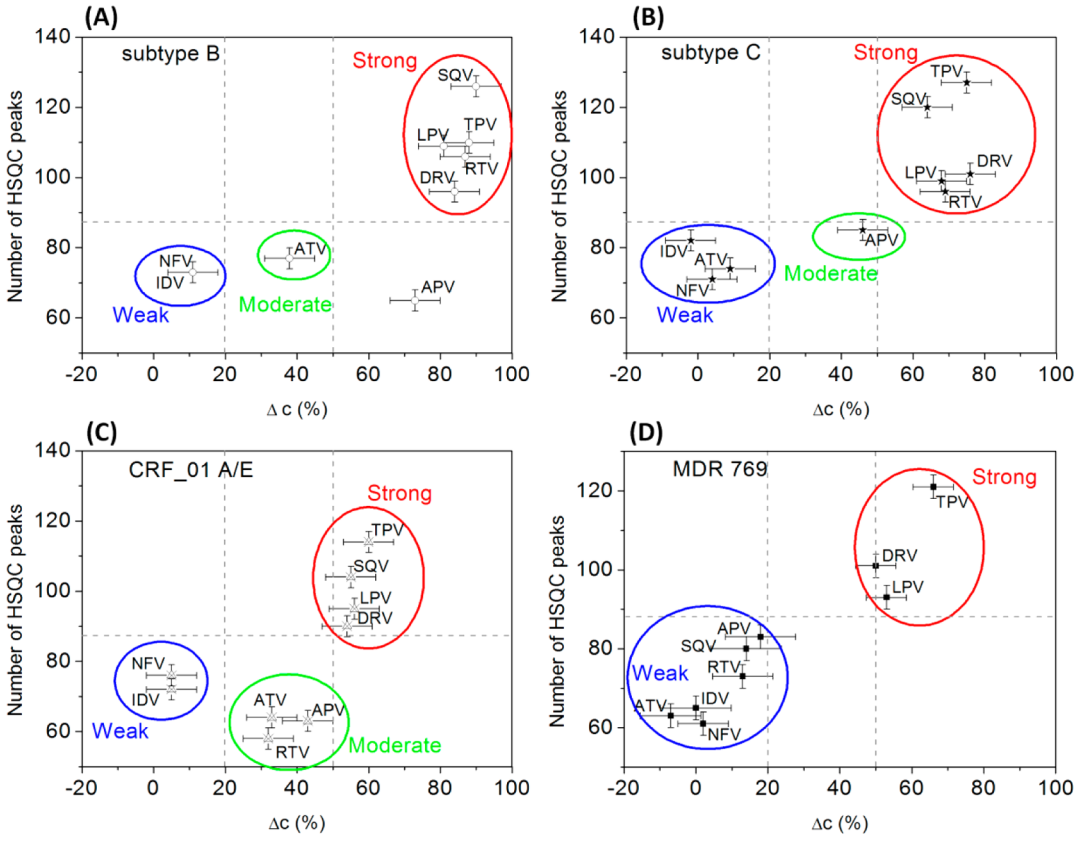

Figure 8. Comparison of number of $^{1}H-^{15}N$ HSQC resonances to changes in fractional occupancy, Δc, induced by inhibitor binding for (A) subtype B, (B) subtype C, (C) CRF_01 A/E, and (D) MDR 769. Error bars are estimated at ±7% for Δc and ±3 for number of HSQC peaks. The horizontal dashed line marks the number of resonances for the apo protease and serves as a demarcation line between fast/intermediate and slow exchange groups, corresponding to the weak/moderate and strong interactions, respectively. The vertical lines indicate borders between weak, moderate, and strong as determined by the DEER results. Data are discussed further within the text.

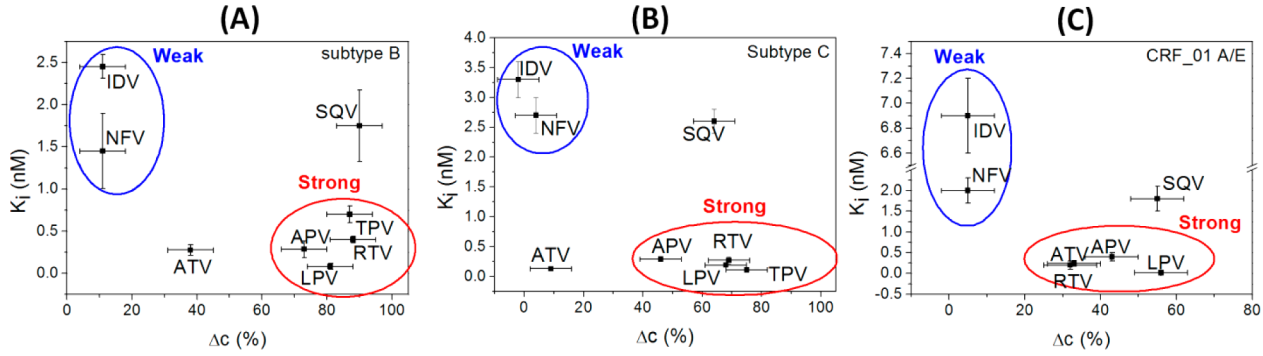

Figure 9. Plots of K_i[38,54] versus Δc for (A) subtype B, (B) subtype C, and (C) CRF_01 A/E. Here, the moderate binding inhibitors are grouped together with the strong inhibitors. SQV is an outlier for all subtypes, with ATV being an outlier for subtypes B and C. Data are discussed within the text. Error bars are estimated at ±7% for Δc and were taken from refs 38 and 54 for K_i values.

residues contribute strongly to the overall inhibitor binding energy, this single mutation does not significantly alter the overall structural binding pattern of the inhibitors, which has been shown for DRV protein complexes with both active and D25N HIV-1 PR.[53] With active enzyme, the FDA-approved inhibitors have dissociation constants, K_d, in the nanomolar range.[12] Introduction of the D25N mutation is known to drop the dissociation constant to the micromolar range.[53] However, the micromolar binding range is perfect for these comparative NMR and EPR studies. If we were to use the active enzyme with inhibitor K_d in the nanomolar range, we would observe strong binding in each case given that the protease concentration in both NMR and EPR experiments is in the micromolar range. To our advantage, the lowered affinity due to the D25N mutation allows for interrogation of how other protein–ligand contacts impact ligand-exchange dynamics and induced population shifts.

To investigate how our results obtained from pulsed EPR and NMR experiments compare to biologically relevant parameters, we plotted values of previously reported inhibition constants of various inhibitors against Δc for subtypes B and C[54] and CRF_01 A/E[38](Figure 9). The results are in general agreement with the nominal categories to which the inhibitors are assigned. The weak inhibitors cluster as one group, whereas

dx.doi.org/10.1021/jp308207h | J. Phys. Chem. B 2012, 116, 14235–14244

the moderate inhibitors bunch together with strong inhibitors. A similar clustering pattern was observed when HSQC peak number was plotted against K_i (Figure S-7, Supporting Information). In this analysis, ATV and SQV are outliers for subtypes B and C, whereas CRF_01 A/E has only SQV as an exception. A possible explanation for this discrepancy might be that, in contrast to the DRV HIV-1PR complexes, D25N substitution might alter the manner in which these inhibitors bind to inactive compared to active enzyme.[52,53] Nevertheless, there is a general similarity of the "groupings" observed, suggesting that the NMR and EPR results with inactive enzyme provide trends that are related to protein−inhibitor interactions in active enzyme but where possible differences are observed with some inhibitors.

CONCLUSIONS

This combined EPR and NMR investigation shows that inhibitors that bind to HIV-1 PR and induce flap closure (i.e, high Δc) undergo slow NMR exchange, indicated by resonance shifts or splitting in $^{1}H-^{15}N$ HSQC titration experiments. This result is understood by considering that slow exchange correlates with a longer residence time of the inhibitor in the active-site pocket, which can be "trapped" during freezing in the DEER experiment. Meanwhile, inhibitors that do not induce substantial flap closure (i.e., low Δc) give HSQC spectra with resonance disappearance or no change, corresponding to intermediate to fast exchange in the NMR time scale or shorter residence time of the ligand in the binding cleft. Overall, the results demonstrate that the presence of glycerol and freezing of the sample does not significantly perturb protein−ligand interactions in HIV-1 PR and provide a framework of how to relate differences in changes of induced conformational shifts among HIV-1 PR constructs with solution protein−ligand interactions, as well as enzymatic inhibition constants.

ASSOCIATED CONTENT

Supporting Information

Further experimental details, protein sequences, data and error analyses, HSQC spectra. This material is available free of charge via the Internet at http://pubs.acs.org.

AUTHOR INFORMATION

Corresponding Author

*E-mail: fanucci@chem.ufl.edu. Tel.: + 1 352 3922345. Fax: + 1 3523920872.

Present Addresses

[‡]Department of Biochemistry & Molecular Biology, University of Massachusetts Amherst, Amherst, MA 01003.

[§]Department of Biochemistry and Molecular Biology, University of Chicago, Chicago, IL 60637.

Notes

The authors declare no competing financial interest.

ACKNOWLEDGMENTS

This work was supported by NSF MBC-0746533 (G.E.F.), NIH R37 AI28571 (B.M.D.), UF Center for AIDS Research, and NHMFL-IHRP. We thank Dr. Alexander Angerhofer and Dr. Joanna R Long for helpful discussions.

REFERENCES

(1) Martinez-Cajas, J. L.; Wainberg, M. A.; Oliveira, M.; Asahchop, E. L.; Doualla-Bell, F.; Lisovsky, I.; Moisi, D.; Mendelson, E.; Grossman, Z.; Brenner, B. G. *J. Antimicrob. Chemother.* **2012**, *67*, 988.

(2) Velazquez-Campoy, A.; Todd, M. J.; Vega, S.; Freire, E. *Proc. Natl. Acad. Sci. U.S.A.* **2001**, *98*, 6062.

(3) Clemente, J. C.; Hemrajani, R.; Blum, L. E.; Goodenow, M. M.; Dunn, B. M. *Biochemistry* **2003**, *42*, 15029.

(4) Rhee, S. Y.; Taylor, J.; Fessel, W. J.; Kaufman, D.; Towner, W.; Troia, P.; Ruane, P.; Hellinger, J.; Shirvani, V.; Zolopa, A.; Shafer, R. W. *Antimicrob. Agents Chemother.* **2010**, *54*, 4253.

(5) Benson, D. A.; Boguski, M. S.; Lipman, D. J.; Ostell, J.; Ouellette, B. F. F. *Nucleic Acids Res.* **1998**, *26*, 1.

(6) *UNAIDS Report on the Global AIDS Epidemic*; Joint United Nations Programme on HIV/AIDS (UNAIDS): Geneva, Switzerland, 2010.

(7) Peeters, M.; Sharp, P. M. *AIDS* **2000**, *14*, S129.

(8) Nkengasong, J. N.; Janssens, W.; Heyndrickx, L.; Fransen, K.; Ndumbe, P. M.; Motte, J.; Leonaers, A.; Ngolle, M.; Ayuk, J.; Piot, P.; Vandergroen, G. *AIDS* **1994**, *8*, 1405.

(9) Vidal, N.; Peeters, M.; Mulanga-Kabeya, C.; Nzilambi, N.; Robertson, D.; Ilunga, W.; Sema, H.; Tshimanga, K.; Bongo, B.; Delaporte, E. *J. Virol.* **2000**, *74*, 10498.

(10) Velazquez-Campoy, A.; Vega, S.; Fleming, E.; Bacha, U.; Sayed, Y.; Dirr, H. W.; Freire, E. *AIDS Rev.* **2003**, *5*, 165.

(11) Bandaranayake, R. M.; Kolli, M.; King, N. M.; Nalivaika, E. A.; Heroux, A.; Kakizawa, J.; Sugiura, W.; Schiffer, C. A. *J. Virol.* **2010**, *84*, 9995.

(12) Velazquez-Campoy, A.; Vega, S.; Freire, E. *Biochemistry* **2002**, *41*, 8613.

(13) Shao, W.; Everitt, L.; Manchester, M.; Loeb, D. D.; Hutchison, C. A., 3rd; Swanstrom, R. *Proc. Natl. Acad. Sci. U.S.A.* **1997**, *94*, 2243.

(14) Kear, J. L.; Blackburn, M. E.; Veloro, A. M.; Dunn, B. M.; Fanucci, G. E. *J. Am. Chem. Soc.* **2009**, *131*, 14650.

(15) Weber, I. T.; Agniswamy, J. *Viruses* **2009**, *1*, 1110.

(16) Galiano, L.; Ding, F.; Veloro, A. M.; Blackburn, M. E.; Simmerling, C.; Fanucci, G. E. *J. Am. Chem. Soc.* **2009**, *131*, 430.

(17) Perryman, A. L.; Lin, J. H.; McCammon, J. A. *Protein Sci.* **2004**, *13*, 1108.

(18) Piana, S.; Carloni, P.; Rothlisberger, U. *Protein Sci.* **2002**, *11*, 2393.

(19) Blackburn, M. E.; Veloro, A. M.; Fanucci, G. E. *Biochemistry* **2009**, *48*, 8765.

(20) Fanucci, G. E.; Cafiso, D. S. *Curr. Opin. Struct. Biol.* **2006**, *16*, 644.

(21) de Vera, I. M. S.; Blackburn, M. E.; Fanucci, G. E. *Biochemistry* **2012**, *51*, 7813.

(22) Jeschke, G.; Polyhach, Y. *Phys. Chem. Chem. Phys.* **2007**, *9*, 1895.

(23) Pannier, M.; Veit, S.; Godt, A.; Jeschke, G.; Spiess, H. W. *J. Magn. Reson.* **2000**, *142*, 331.

(24) Kim, M.; Xu, Q.; Murray, D.; Cafiso, D. S. *Biochemistry* **2008**, *47*, 670.

(25) Georgieva, E. R.; Roy, A. S.; Grigoryants, V. M.; Borbat, P. P.; Earle, K. A.; Scholes, C. P.; Freed, J. H. *J. Magn. Reson.* **2012**, *216*, 69.

(26) Galiano, L.; Bonora, M.; Fanucci, G. E. *J. Am. Chem. Soc.* **2007**, *129*, 11004.

(27) Galiano, L.; Blackburn, M. E.; Veloro, A. M.; Bonora, M.; Fanucci, G. E. *J. Phys. Chem. B* **2009**, *113*, 1673.

(28) Tsvetkov, Y. D.; Grishin, Y. A. *Instrum. Exp. Tech.* **2009**, *52*, 615.

(29) Jeschke, G.; Chechik, V.; Ionita, P.; Godt, A.; Zimmermann, H.; Banham, J.; Timmel, C. R.; Hilger, D.; Jung, H. *Appl. Magn. Reson.* **2006**, *30*, 473.

(30) Jeschke, G.; Panek, G.; Godt, A.; Bender, A.; Paulsen, H. *Appl. Magn. Reson.* **2004**, *26*, 223.

(31) Swanson, M. A.; Kathirvelu, V.; Majtan, T.; Frerman, F. E.; Eaton, G. R.; Eaton, S. S. *J. Am. Chem. Soc.* **2009**, *131*, 15978.

(32) Delaglio, F.; Grzesiek, S.; Vuister, G. W.; Zhu, G.; Pfeifer, J.; Bax, A. *J. Biomol. NMR* **1995**, *6*, 277.

(33) Huang, X.; de Vera, I. M.; Veloro, A. M.; Rocca, J. R.; Simmerling, C.; Dunn, B. M.; Fanucci, G. E. *Biomol. NMR Assign.*, published online Jul 1, 2012, http://www.dx.doi.org/10.1007/s12104-012-9409-7.
(34) Ding, F.; Layten, M.; Simmerling, C. *J. Am. Chem. Soc.* **2008**, *130*, 7184.
(35) Torbeev, V. Y.; Raghuraman, H.; Mandal, K.; Senapati, S.; Perozo, E.; Kent, S. B. *J. Am. Chem. Soc.* **2009**, *131*, 884.
(36) Torbeev, V. Y.; Raghuraman, H.; Hamelberg, D.; Tonelli, M.; Westler, W. M.; Perozo, E.; Kent, S. B. H. *Proc. Natl. Acad. Sci. U.S.A.* **2011**, *108*, 20982.
(37) Coman, R. M.; Robbins, A. H.; Goodenow, M. M.; Dunn, B. M.; McKenna, R. *Acta Crystallogr. D: Biol. Crystallogr.* **2008**, *D64*, 754.
(38) Clemente, J. C.; Coman, R. M.; Thiaville, M. M.; Janka, L. K.; Jeung, J. A.; Nukoolkarn, S.; Govindasamy, L.; Agbandje-McKenna, M.; McKenna, R.; Leelamanit, W.; Goodenow, M. M.; Dunn, B. M. *Biochemistry* **2006**, *45*, 5468.
(39) Scott, W. R.; Schiffer, C. A. *Structure* **2000**, *8*, 1259.
(40) Hornak, V.; Okur, A.; Rizzo, R. C.; Simmerling, C. *Proc. Natl. Acad. Sci. U.S.A.* **2006**, *103*, 915.
(41) Sadiq, S. K.; De Fabritiis, G. *Proteins* **2010**, *78*, 2873.
(42) Toth, G.; Borics, A. *J. Mol. Graph. Model.* **2006**, *24*, 465.
(43) Rick, S. W.; Erickson, J. W.; Burt, S. K. *Proteins* **1998**, *32*, 7.
(44) Spinelli, S.; Liu, Q. Z.; Alzari, P. M.; Hirel, P. H.; Poljak, R. J. *Biochimie* **1991**, *73*, 1391.
(45) Meiselbach, H.; Horn, A. H. C.; Harrer, T.; Sticht, H. *J. Mol. Model.* **2007**, *13*, 297.
(46) Kear, J. L.; Galiano, L.; Veloro, A. M.; Busenlehner, L. S.; Fanucci, G. E. *J. Biophys. Chem.* **2011**, *2*, 137.
(47) Kempf, J. G.; Loria, J. P. *Cell Biochem. Biophys.* **2003**, *37*, 187.
(48) Freedberg, D. I.; Ishima, R.; Jacob, J.; Wang, Y. X.; Kustanovich, I.; Louis, J. M.; Torchia, D. A. *Protein Sci.* **2002**, *11*, 221.
(49) Logsdon, B. C.; Vickrey, J. F.; Martin, P.; Proteasa, G.; Koepke, J. I.; Terlecky, S. R.; Wawrzak, Z.; Winters, M. A.; Merigan, T. C.; Kovari, L. C. *J. Virol.* **2004**, *78*, 3123.
(50) Wang, Y.; Liu, Z.; Brunzelle, J. S.; Kovari, I. A.; Dewdney, T. G.; Reiter, S. J.; Kovari, L. C. *Biochem. Biophys. Res. Commun.* **2011**, *412*, 737.
(51) Panchal, S. C.; Pillai, B.; Hosur, M. V.; Hosur, R. V. *Curr. Sci.* **2000**, *79*, 1684.
(52) Katoh, E.; Louis, J. M.; Yamazaki, T.; Gronenborn, A. M.; Torchia, D. A.; Ishima, R. *Protein Sci.* **2003**, *12*, 1376.
(53) Sayer, J. M.; Liu, F. L.; Ishima, R.; Weber, I. T.; Louis, J. M. *J. Biol. Chem.* **2008**, *283*, 13459.
(54) Coman, R. M.; Robbins, A. H.; Fernandez, M. A.; Gilliland, C. T.; Sochet, A. A.; Goodenow, M. M.; McKenna, R.; Dunn, B. M. *Biochemistry* **2008**, *47*, 731.